



# Fuzzy Clustering Based Image Denoising and Improved Support Vector Machine (ISVM) Based Nearest Target for Retina Images

B. Sivaranjani, C. Kalaiselvi

**Abstract:** A developing automated retinal disease diagnostic system based on image analysis has now demonstrated the ability in clinical research. Though, the accuracy of these systems has been negotiated repeatedly, generally due to the basic effort in perceiving the abnormal structures as well as due to deficits in the image gaining that affects image quality. Use the fuzzy clustering; the noises contained in the samples are omitted from the above. Unless the noises will be taken away from the samples instead dimension reduction initializes the optimization of Mutual Information (MI) as just a coarse localization process that narrows the domain of optimization and tries to avoid local optimization. Furthermore, the suggested work closer to the retina picture being done using the Improved Support Vector Machine (ISVM) system used in the area-based registration, offering a reliable approach. It is the first matching template algorithm for retina images with tiny template images of unconstrained retinal areas to the best understanding.

**Keywords:** Retina image template matching, Noise removal, Fuzzy clustering, Improved Support Vector Machine, teleophthalmology, dimension reduction, mutual information, health monitoring.

## I. INTRODUCTION

Teleophthalmology is becoming increasingly important as an efficient way to deliver eye care worldwide. Teleophthalmology is used in many developing countries to provide all the underprivileged urban population and the remote rural population with reliable eye care. Technological innovations have strengthened proof over the years, and teleophthalmology has developed from such a learning tool to a clinical device. Teleophthalmology provides the same optimal therapeutic outcome as traditional system. Remote portals empower clinicians should provide treatment across a larger area, thus improving quality of life outcomes and growing accessibility to a larger population of specialty care. Leading to increased accessibility and decreased commuting costs and time, a high level of satisfaction and acceptance is recorded in most studies. Given the documented increased quality of patient safety and patient satisfaction for all these programs in telemedicine, this analysis examines how teleophthalmology greatly improves health outcomes.

Teleophthalmology offers an easy and value-effective way to detect many retinal diseases and eventually to preserve the eyesight of a patient. In the retina, there has also been a trend toward more teleophthalmology,

Particularly in areas in which retinal specialists may not be easily available for diabetic retinopathy and premature retinopathy (ROP) screening. In this section, the difficult issue of matching and recording retinal images was discussed to allow for new applications for teleophthalmology. A new technique for locating optic discs in retinal images was suggested in [1].

The first phase of certain vessel segmentation, disease diagnosis, and retinal recognition algorithms would be to locate the optic disc and its core. In [2] the latest research on the essential characteristics and features of DR eye telehealth services was evaluated in the categories listed: image gradability, mydriasis, sensitivity and specificity, cost-effectiveness, long-term efficacy, patient comfort and satisfaction, and patient-related results change. In [3] analyzed recent trends in DR screening imaging and new technologies, showing potential for growth on existing approaches to screening.

In [4] the value-benefit analysis to use a digital retinal imaging assessment based on telemedicine was examined, compared to conventional diabetic retinopathy evaluation of diabetic patients. The economic impact of eye care telemedicine in a mountainous, rural health center in West Virginia over a period of seven years from 2003-2009 was evaluated in [5]. In [6] established if proliferative diabetic retinopathy (PDR) screening of tele-ophthalmology could be price-saving. In [7], it was proposed that primary care hospitals may use telemedicine to monitor for diabetic retinopathy and track for disease intensifying over a prolonged period of time. In [8], patient preference for diabetic retinopathy (DR) screening is evaluated with teleophthalmology or face-to-face ophthalmology in Nairobi, Kenya. In [9] the history about using telemedicine technology to assess ophthalmology in diabetic and hypertensive cases reporting to a community clinic in rural West Virginia was identified.

In [10], the ability to assess non-diabetic retinal observations in diabetes patients either using non-mydratic fundus photography (NMFP) or Ultra Wide Field Imaging (UWFI) into a known teleophthalmology program was compared using verified retinal imaging methods. In [11], a method was suggested to identify in retinal images of objects and to mask the affected areas in order to prevent them from being regarded for the automatic detection of retina diseases.

Manuscript published on January 30, 2020.

\* Correspondence Author

**B. Sivaranjani\***, Assistant Professor, Department of Computer Science, Dr. N. G. P. Arts and Science college, Coimbatore (TN) India.

**Dr. C. Kalaiselvi**, Head and Professor, Department of Computer Applications, Tirupur Kumaran College for Women, Tirupur (TN) India.

© The Authors. Published by Blue Eyes Intelligence Engineering and Sciences Publication (BEIESP). This is an [open access](http://creativecommons.org/licenses/by-nc-nd/4.0/) article under the CC-BY-NC-ND license (<http://creativecommons.org/licenses/by-nc-nd/4.0/>)

In [12] the cost-effectiveness of a rural Southern India telemedicine diabetic retinopathy (DR) screening system conducting 1-off screening camps (i.e. screening provided once) in villages was assessed and the actual cost-effectiveness proportions of different screening intervals were assessed. In [13] an innovative telehealth method illustrated accuracy that can enhance the diagnostic process for ASD; but, there are drawbacks which should be acknowledged while interpreting the results.

- In [14] the efficacy and acceptance of ADSs to facilitate child learning through the everyday play and care experiences of families at home was examined. In [15] the reliability and feasibility of telehealth language assessments for children with autism in school age were assessed. The findings indicate that, under certain conditions, telehealth may pose an effective and feasible approach to assessing language for children with autism as a main or a substitute service model, whereas recognizing that differences between these children might be important to take into account when preparing both telehealth evaluation and intervention. It provides the eye with a remarkable opportunity to view in vivo internal biological tissues, and several diseases could be detected and monitored by means of ocular imaging. For this motivation, the early diagnosis of autism disorder has been concentrated on the prompt identification of autism pathological changes through regular retinal screening and analysis in this work. The work's principal contribution is as follows:
- The input retina image has been denoised to use fuzzy clustering, in which the fuzzy c-means are implemented in the detection process, providing an ideal grouping of noisy data and incorruptible image data to retain the visual information as well.
- The coares localization process is carried out by using Mutual Information to determine the closest target image throughout the low-dimensional space and to record the nearest target image with MI
- In order to match the template, the improved support vector machine has been extended by locating the closest target image as well as the end result of the diagnostic process of diseases is done.

The rest of the research is organized as follows: an effective and accurate retinal matching technique is proposed and explained in section 2 that incorporates dimension reduction and mutual information (MI) with a pre-processing method of fuzzy c-means clustering with ISVM. The experimental results are discussed in section 3 with a comparison between the existing and proposed method. Finally, section 4 reveals the conclusion with the future work.

## II. ISVM BASED TEMPLATE MATCHING OF RETINA IMAGES

Retina images managed to capture through an adapter-based optics offer better information and low image quality, that further rises template matching difficulty. The input retina images are denoised utilizing fuzzy c-means clustering method to solve the problem. Afterwards, the principal component analysis (PCA) used it to roughly locate the image of the template, so the consequent displacement parameters will be used to initialize the metric optimization

of Mutual Information (MI), and that is the initial parameters given by the coarse location in the MI metric convergence domain. A further contribution would be that this article enacts an efficient Improved Support Vector Machine (ISVM) to accelerate the matching of overlapping images between unordered data, the automated method of matching retina limits and registry used in the sophisticated teleophthalmology and long-term retinal monitoring. Fig.1 shows the overall description of the proposed work.

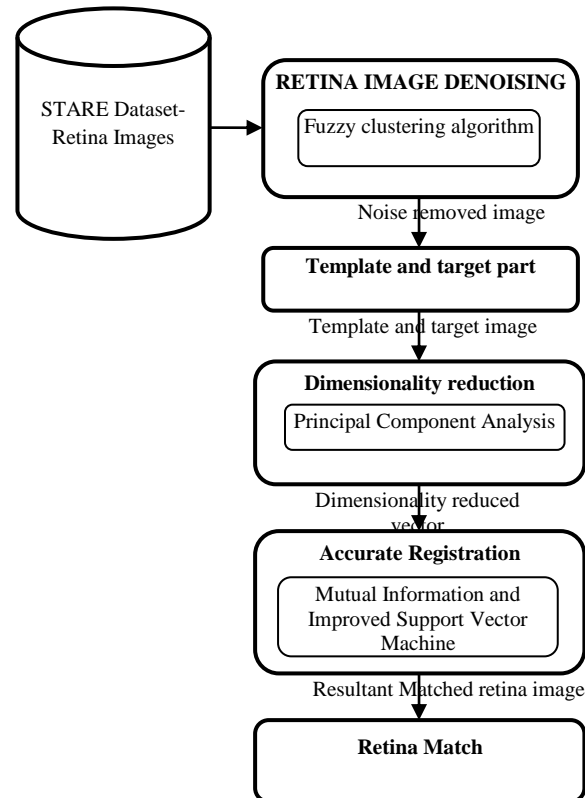
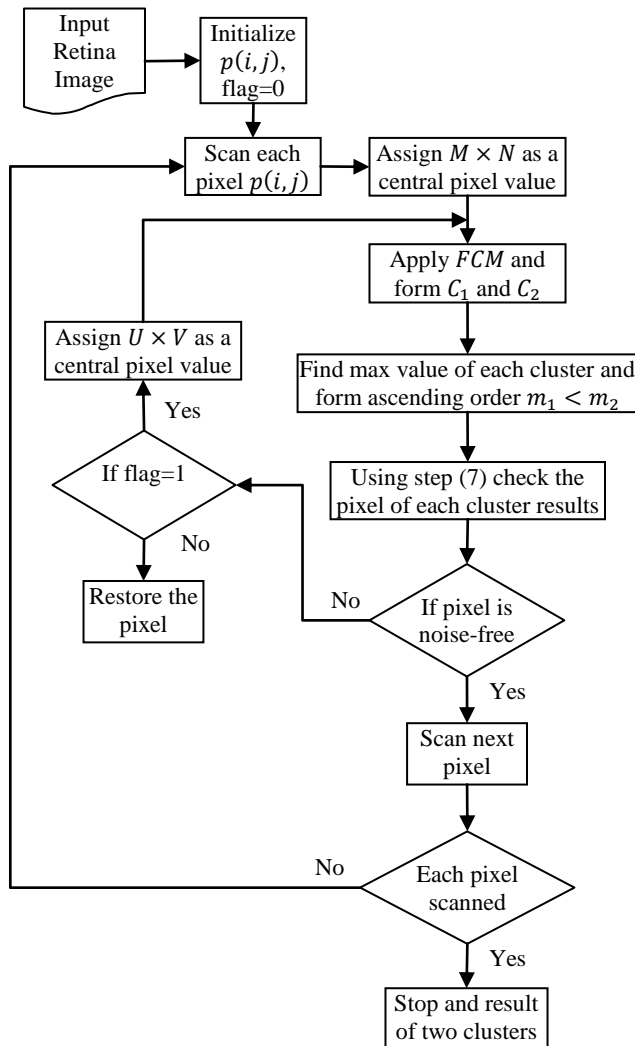


Fig.1. Overall Proposed Retina Matching Process

### A. Retina Image Preprocessing Using Fuzzy Clustering

Retina Dataset: The suggested approach has tested with synthetic deformations on the STARE retinal dataset [21] and in vivo data collected by an optical system D-eye based on a low-cost (< US\$ 400) adapter. On the STARE dataset, the performance of various dimensional reduction techniques is also compared. Fig.2 displays the flowchart of the proposed retina picture that denounces the use of fuzzy clustering.



**Fig.2.The Flowchart of Proposed Retina Image Denoising Using Fuzzy Clustering**

Effective noise removal depends primarily on the identification phase. The proposed algorithm's detection method effectively determines the location of noisy pixels, thus raising the false alarm rate and the rate of miss detection. The high intensity and low intensity noisy pixels come clustered independently using clustering. The majority of the pixels are in the noise-free group. The detection of impulse noise has been accomplished in two processes in this noise removal technique, first locating the noisy pixels and second maintaining the noise-free pixel value shown in Fig.3.

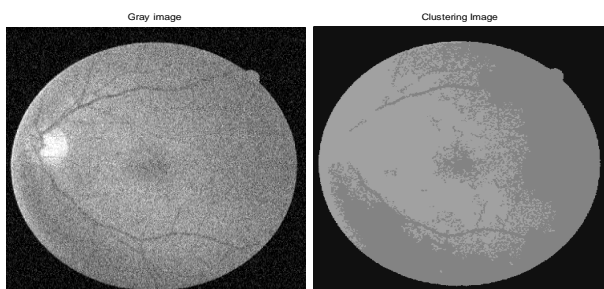


**Fig.3.Fuzzy Clustering Noise removal**

**The step by step process of Image denoising process:**

1. **Process I: Location of noisy pixels detection**
2. Select a window size  $M \times N$  that can be centered on each pixel of retina image.

3. Let the central pixel at which window is centered be  $p(i,j)$  using FCM algorithm, divide the neighborhood values of the central pixel into two clusters.
4. Let the two clusters formed after applying FCM be  $C_1$  and  $C_2$ . After the formation of clusters find the maximum value present in each cluster respectively.
5. In window there will be  $M \times N = X$  values. The FCM algorithm divides these  $X$  values unsupervisedly into two clusters. Let the two maximum values present in these clusters be  $m_1$  and  $m_2$ .
6. Then  $m_1$  and  $m_2$  values from each cluster are sorted in ascending order, such that  $m_1 < m_2$ .
7. Using the following equation, check whether the central pixel  $p(i,j)$  is noisy or noise-free.

$$p(i,j) = \begin{cases} \text{noise} & \text{if } p(i,j) \leq m_1 \\ \text{noise free} & \text{if } m_1 < p(i,j) \leq m_2 \end{cases}$$

Where, pixels in the cluster having the minimum, maximum value i.e.  $m_1$  are lowest intensity pixels which contain the noise. The cluster having the maximum value as  $m_2$  is considered as noise free cluster.

8. If the pixel lies in a noise free cluster, it is left unaltered.
9. If the pixel is noisy it is processed again in the second detection stage.

#### 10. Process II: Location of noisy pixels detection

11. Now change the window size to  $U \times V$
12. Repeat Steps 3-7 in the same way up to the stopping criteria is met
13. If the pixel is detected as a noisy pixel in the second detection stage also, it is marked as noisy pixel else noise free.
14. Restoration of noisy pixels is performed using the well known median filter. Median value for neighbouring pixels within the window of size  $U \times V$  is computed and is used to replace the noisy pixel value.

#### B. PCA for Location Estimation and Mutual Information

The combination of dimensionality reduction and image registration based on mutual knowledge in this section. After denoising the image, methods of dimension reduction enable low-dimensional summaries to be constructed when removing redundancies and noise in the data. The full image dimension has been duplicated to estimate the location of the template in the 2d space, hence dimensional reduction methods added to the coarse location of the template. In this segment, as it is simple and flexible, PCA is chosen as the Retina Match dimension reduction method. A broad-field fundus image or a mosaic image from D-eye images can be the full image. In particular, as a weighted linear combination of input variables, PCA creates a range of new variables as well as the detailed description is defined in [17].

The maximization of MI for the registration of multimodal images is specified afterwards.



A wide-field fundus image or a mosaic image from D-eye images could be the full image. The optimizer used it to maximize the MI is based on the approach used by Newton. The MI function has become a quasi-concave function, and the Newton's method parabolic theorem is valid only near convergence. It will induce the optimization to diverge once the initial transformation takes place on the convex portion of the cost functions. The suggested coarse localization gives a good configuration of the displacement to maximize the cost function of the MI subsequently. The calculation is similar to the optimum value and drops within the MI metric's convex domain, offering more effective optimization and avoiding extreme position. The basic concept is to first use PCA and blocking PCA for coarse position that can be a warm beginning to pursue correct registration is shown in Fig.4.

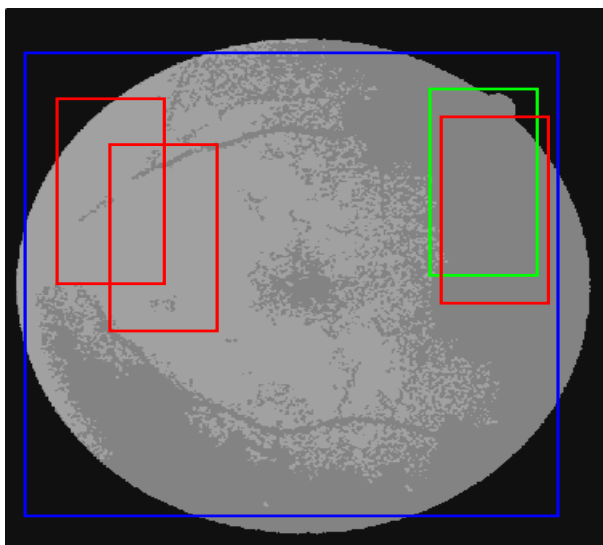


Fig.4.PCA and Coarse Localization

To discover the optimal transformation, the MI metric has been configured for accurate registration. After the optimization domain is reduced to a narrow range close to the optimal position with coarse localization, high precision and efficiency could be achieved by accurate registration. Fig.5 shows the coarse location

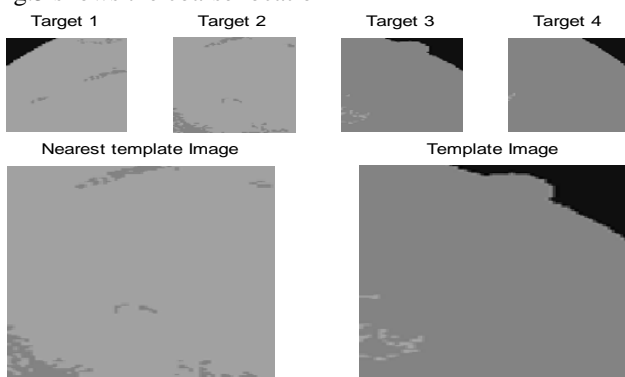


Fig.5.The coarse localization with nearest target image

### C. Proposed Template Matching Using ISVM

Many of the basic works on the matching of retinal images with models are based on the more general methods of image registration, that have been studied extensively in recent times. Nevertheless, general methods for registering retina focus on matching pairs of images that also have a

large FOV with local deformities or different modalities of the image as shown in Fig.6.

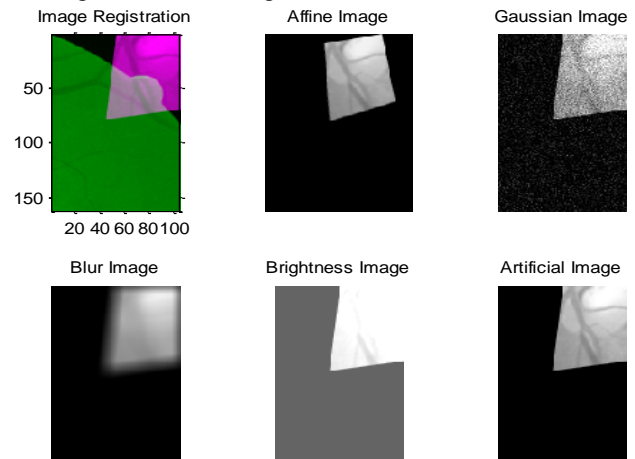


Fig.6.Image Registration

A current template matching method utilizing ISVM has been implemented in this segment to deal with the challenges presented by recording small FOV and low-quality retinal images on a full image by stitching as demonstrated in Fig.7. The template matching classifier operates on a set of templates, i.e. super vectors that could be characterized a priori or chosen by the user once the ISVM detects an abnormal sound.

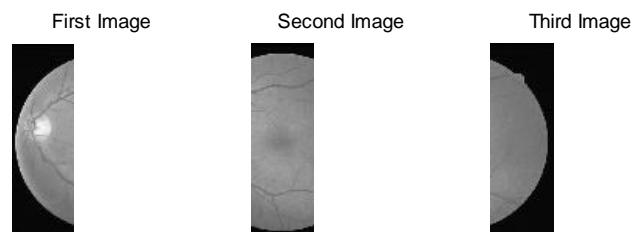


Fig.7.Image Stitching

Signifying through  $x$  the super vector of the input retinal images with  $Y = y_1, \dots, y_N$  the set of templates, the algorithm works by estimating the Euclidean distance  $D^{(i)} = \|x - y_i\|$  between super vector and all templates throughout the set. Signifying the super vector  $x$  with  $D_{\min} = D^i$ , is classed as a fall if  $D_{\min} > \beta$  and otherwise as a non-fall. The threshold seems to be an algorithm's hyper parameter which can be set on a validation set. Support Vector Machine (SVM) is intended to adapt to the new datasets, two or more classifiers of any kind.

The question is how to choose the right adaptation classifier. The solution to the issue is to choose the parameter classifier after assessing each classifier's performance on a sparingly labeled dataset.

The overall problem of the binary classification task is regarded in the original STARE retina image dataset  $D$ , that consists of most unlabeled instances  $D_u$  and a limited number of labeled instances  $D_l$ , so the original dataset is  $D=D_uD_l$ : there is one or even more subordinate  $D_{ks}$  datasets that differ from the original dataset. The  $f_k$  subordinate classifier is being used to train each of the  $D_{ks}$  and  $D_l=x_i, y_i=1$  subordinate datasets, where  $x_i$  is the vector of the  $i$ th data and  $y_i=1$  is its binary number. The data vector often contains a constant 1 as its first variable, so  $d$  is the number of features,  $x_iRd+1$ .

There exist multiple subordinate datasets as  $D_{ks}, \forall k=1, \dots, m$  with  $D_{ks}=x_{ik}, y_{ik}N_k$ . The subordinate dataset description is different from the original dataset. The subordinate classifier  $f_k$  have been trained from each subordinate dataset, which gives us the result of prediction of data label through the sign of its decision function, i.e.  $y=f_kx$ . The traditional SVM trains the from the labeled dataset  $D_l$ . ISVM is used to adapt a combination of multiple existing classifiers  $f_{ks}, k=1, \dots, m$  to the new classifier. The traditional SVM trains the  $f_k$  from the labeled dataset  $D_l$ . The decision boundary is determined by the kernel function  $x, x'=x, x'$ , where  $x$  is a feature vector. The kernel function is the inner product of two projected feature vectors. Delta function is used in ISVM in the form of  $f_kx=wT_x$  on the basis of  $f_kx$ , where,  $w$  are the parameters predicted from the labeled data  $D_l$ .

As defined earlier, the objective is to make a group of subordinate classifiers and adapt this group to new classifier  $f(x)$ ,  $f(x) = \sum_{k=1}^m t_k f_k(x) + \Delta f(x)$  Where,  $t_k \in [0,1]$  is the weight of each subordinate classifier  $f_k(x)$  which sums to one as .

1. **INPUT:** Input supervector  $x$ ,  $y = \{y_1, \dots, y_N\}$ , label information, Error threshold = Huge value
2. **OUTPUT:** Set of support vectors,
3. Map images into space  $Z = xW$
4. For each image  $X_i$
5. Find the nearest 3 neighbors  $x$  minimizing the feature distance using Euclidean  $d(Z_i, Z_j)$
6. Compute the Mutual Information between each  $x_j$  and  $x_i$  and take the adjacent image with highest MI.
7. Begin:
8. Randomly sample 2 points belonging to different classes are defined as  $f_k(x)$ . Add the  $m$  to the current set of support vectors.
9. Set the corresponding dual variables-“ $\alpha$ ” values
10. ISVM ()
11. {
12. LOOP Forever
13. LOOP to randomly sample 40 points.
14. Choose the set of 40 points with which current SVs give 40 pt test error less than the current error threshold.
15. Calculate kernel function to find the decision boundary
16. BREAKIF Points are insufficient.
17. ENDLOOP Random sampling of 40 points
18. BREAKIF the Inner LOOP is at QUIT because of insufficient points.
19. Update error threshold as the average of 40 pt test errors.
20. LOOP Over misclassified points.
21. Add the point to current SVs.
22. Train using ISVM with a warm start and test over the remaining points.

23. ENDLOOP over misclassified points.
24. ADD the misclassified point that gave the min-most error to the SVarray over the remaining points.
25. Save dual variable “ $\alpha$ ” s for the next iteration end loop FOREVER.
26. ISVM (); // SVM with kernel function
27. END.
28. Panorama R Mosaicking: Align all the adjacent images with mutual information based registration method.
29. Panorama blending.
30. return panorama R

Using these two parameters for input parameters before joining the classification algorithm. The adjacent images can therefore be effectively identified and registered. We create the matrix  $x$  for a series of small images  $x$ , as with the matrix  $T$ . Of each image  $I$  like shown in Fig.8, PCA has been extended to  $x$  and reverts the lower-dimensional features. PCA is applied to  $x$  and returns the low-dimensional features for each image  $i$  as shown in Fig.8.

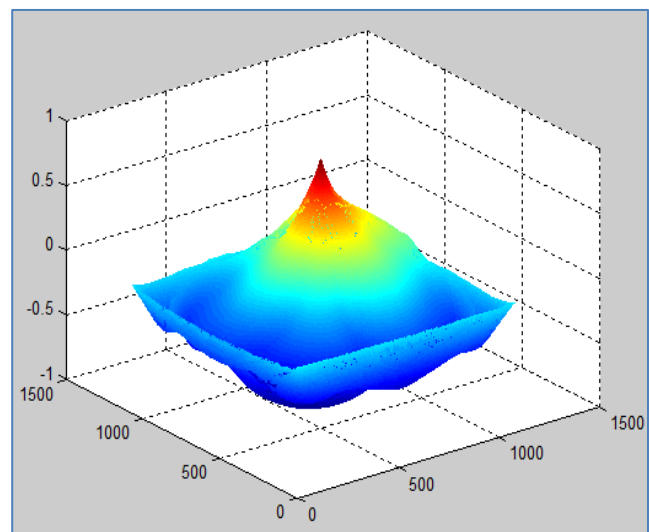
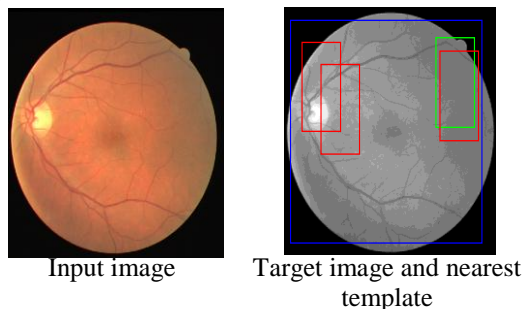


Fig.8.Low dimensional Block PCA

In  $I$ , the distance between features shows the distance between images. Image  $x_i$  s closest neighbor  $x_j$  is the one with the greatest overlap; the pair of images is then reported with MI-based approach. To enhance the robustness of the algorithm, the 3-nearest neighbors are then chosen for each image to calculate MI, and the one with the highest metric value is maintained. The ISVM algorithm is intended to help classify multi-image as a recursive function. It is possible to get more than one image during most of the testing time. The function of ISVM is termed iteratively and specifies all images with the output. The picture will be marked as affected or not affected on first call. The call provides the disease grade for affected images, input parameters are cotton wool spots and vein pixels removed. We can build models (database) for trained images using these two parts and set a clear classification of a test time. Simply tag the output to read "affected with (the grade of the disease)" or "not affected."

### III. EXPERIMENTAL RESULTS AND DISCUSSION

The experimental results are performed among three matching methods using retinal images in ASIFT [18] and RetinaMatch [17]. The images of full fund us from the STARE dataset are retrieved on matching image of four hundred source fund us images as strong and sick retinas. Every image pair holds a full fund us image on random selection on mapping after affine transformation from a square into a parallelogram. Cropping of square mapped in this area as well as warping is done to get square template. 200×200 pixels size is attained in The FOV template images for 12 images. The template dimension is 10% of the full image. The Mutual Information output of the developed MI-SVMs are analysed along prevailing methods such as IR-MI and MI for five types of methods such as Affine, Gaussian, Blur, Brightness and Artificial. The input of retina image with Target Image and Nearest Template is shown in Fig.9.



**Fig.9. Retina image with Target Image and Nearest Template**

#### 1. Image Recognition comparison of Proposed MI-ISVM

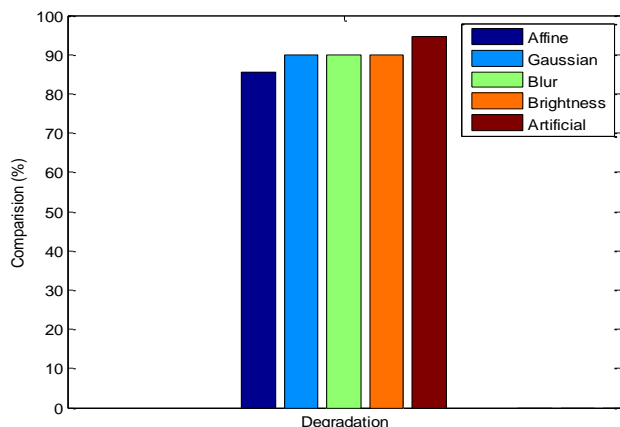


**Fig.10. Result of Image matching-MI-ISVM**

From the above Fig.10, the graph explains that the degradation comparison for the five type of images such as Affine, Gaussian, blur, brightness and artificial images in specified datasets. The method MI-ISVM-image recognition (MI-SVM) with degradation result is illustrated in Figure.4. When number of degradation increased according with the comparison of IR value is increased. From this graph, it is learnt that the proposed MI-SVM provides higher comparison result for artificial images which produce better template matching results. The reason is that the fuzzy clustering produce the noise free images which will improve the nearest target detection results.

#### 2. Image recognition comparison of Mutual Information (IR-MI)

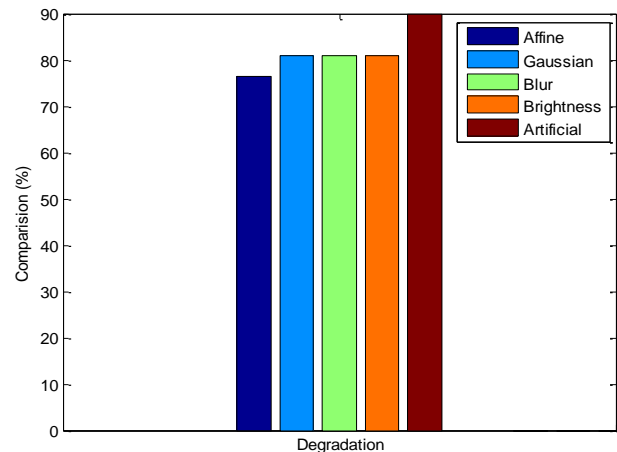


**Fig.11. Result of Image matching-Recall Rate**

From the above Fig.11, the graph explains that the degradation comparison for the five type of methods such as Affine, Gaussian, blur, brightness and artificial in specified datasets with IR results. The method mutual information-image recognition (IR-MI) with degradation result is illustrated in Figure.11. When number of degradation increased according with the comparison of IR value is increased. From this graph, it is learnt that the proposed IR-MI provides higher comparison result for artificial methods which produce better template matching results.

#### 3. Comparison of IR-MI and IR-SVM

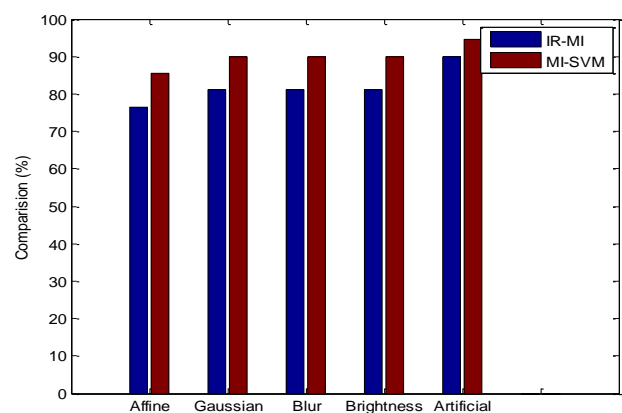


**Fig.12. Result of Retina matching-IR-MI and MI-SVM**

From the above Fig.12, the graph explains that the f-measure comparison for the number of methods such as Affine, Gaussian, blur, brightness and artificial in specified datasets. The methods are executed such as IR-MI and MI-SVM. The number of images is increased and the comparison value is increased correspondingly. From this graph it is learnt that the proposed MI-SVM provides higher comparison result of 94.5% for artificial and than the previous method of IR-MI at the value of 90%. Thus the proposed ISVM algorithm is greater in terms of better template matching results. The reason that the kernel function of SVM is improved with delta function which will improve the fetching template matching results.



The numerical results of IR-MI and MI-SVM is given in Table.1.

**Table - I. Numerical Results of IR-MI and MI-SVM**

Method	IR-MI	MI-SVM
Affine	76.5	85.5
Gaussian	81	90
Blur	81	90
Brightness	81	90
Artificial	90	94.5

### 1.1. Comparison of MI,IR-MI and IR-SVM

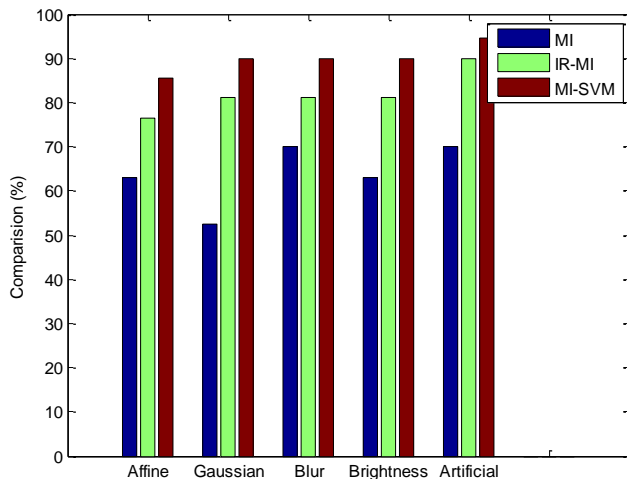


**Fig.13.Retina matching MI, IR-MI and MI-SVM**

From the above Fig.13, the graph explains that the processing time comparison for the number of images in specified datasets. The methods are executed such as MI, IR-MI and MI-SVM. In x-axis the five methods such as Affine, Gaussian, blur, brightness and artificial is considered and in y-axis the accuracy value is considered. From this graph it is learnt that the proposed MI-SVM provides high comparison result at the artificial method of 94.5%, IR-MI is 90% and MI is 70%. Thus the output explains that the proposed MI-SVM algorithm is greater to the existing algorithms in terms of better template matching results with high accuracy rate. The reason is that existing approaches has a low rate of triumph that attaining maximum probability for mis-detection clarification on emergency. Table 2 explores the mean error rate, success rate and run time rate in number. The minimum error rate is attained in MI-SV and depicted with 0.30, high success rate of 81 and low run time rate of 0.19.

**Table - II. Numerical result of mean error rate, success rate and run time rate**

Values	MI	IR-MI	MI-SVM
Mean Error	1.32	0.70	0.30
Success Rate	63	75.43	81
Run Time	1.46	0.335	0.19

### IV. CONCLUSION AND FUTURE WORK

As conclusion, Retina Match methodology is achieved with base fact of ISVM and fuzzy concept that supports in remote retina health monitoring along devices for capturing images.

Thence, FCM application determines pixels as noisy by a familiar technique Retina Match algorithm. MI based registration is provided for template registration on PCA-based coarse localization with better initialization. the images that is being captured onto the full retina image are performed along ISVM, the hemorrhagic spots for ease segmentation on deleting instant retinal area and prevailing instance. Thence, Retina Match is attained for affine transformation with better accuracy among image pair for low quality and a enhanced FOV baseline. From experimental results and analyses part on ASIFT and RetinaMatch, it is proven that developed algorithm attains higher performance. Further, better restoration might be included along the efficient detection scheme via machine learning methods.

### REFERENCES

- Dehghani, Amin, Hamid AbrishamiMoghaddam, and Mohammad-ShahramMoin. "Optic disc localization in retinal images using histogram matching." EURASIP Journal on Image and Video Processing 2012, no. 1 (2012): 19.
- Aditi Gupta, Jerry Cavallerano, Jennifer K. Sun & Paolo S. Silva (2017) Evidence for Telemedicine for Diabetic Retinal Disease, Seminars in Ophthalmology, 32:1, 22-28.
- Rachapelle S, Legood R, Alavi Y, et al. The cost-utility of telemedicine to screen for diabetic retinopathy in India. Ophthalmology 2013;120(3):566-573.
- Li Z, Wu C, Olayiwola JN, Hilaire DS, Huang JJ. Telemedicine-based digital retinal imaging vs standard ophthalmologic evaluation for the assessment of diabetic retinopathy. Conn Med.2012;76(2):85-90.
- Richardson DR, Fry RL, Krasnow M. Cost-savings analysis of telemedicine use for ophthalmic screening in a rural Appalachian health clinic. W V Med J. 2013;109(4):52-55.
- Brady CJ, Villanti AC, Gupta OP, Graham MG, Sergott RC. Tele-ophthalmology screening for proliferative diabetic retinopathy in urban primary care offices: An economic analysis. Ophthalmic Surg Lasers Imaging Retina. 2014;45(6):556-561.
- Mansberger SL, Sheppler C, Barker G, et al. Long-term comparative effectiveness of telemedicine in providing diabetic retinopathy screening examinations: A randomized clinical trial. JAMA Ophthalmology 2015;133(5):518-525.
- Kurji K, Kiage D, Rudnisky CJ, Damji KF. Improving diabetic retinopathy screening in Africa: Patient satisfaction with teleophthalmology versus ophthalmologist-based screening. Middle East Afr J Ophthalmol. 2013;20(1):56-60
- Ahmed R, Petrany S, Fry R, Krasnow M. Screening diabetic and hypertensive patients for ocular pathology using telemedicine technology in rural West Virginia: A retrospective chart review. W V Med J. 2013;109(1):6-10.
- Silva PS, Cavallerano JD, Haddad NM, et al. Comparison of nondiabetic retinal findings identified with nonmydriatic fundus photography vsultrawide field imaging in an ocular telehealth program. JAMA Ophthalmology. 2016;134(3):330-334.
- Mora, André D., JoãoSoares, and José M. Fonseca. "A template matching technique for artifacts detection in retinal images." In 2013 8th International Symposium on Image and Signal Processing and Analysis (ISPA), pp. 717-722. IEEE, 2013.
- Rachapelle, S., Legood, R., Alavi, Y., Lindfield, R., Sharma, T., Kuper, H. and Polack, S., 2013. The cost-utility of telemedicine to screen for diabetic retinopathy in India. Ophthalmology, 120(3), pp.566-573.
- Smith, Christopher J., AgataRozga, Nicole Matthews, Ron Oberleitner, NazneenNazneen, and Gregory Abowd. "Investigating the accuracy of a novel telehealth diagnostic approach for autism spectrum disorder." Psychological assessment 29, no. 3 (2017): 245
- Vismara, Laurie A., Gregory S. Young, and Sally J. Rogers. "Telehealth for expanding the reach of early autism training to parents." Autism research and treatment 2012 (2012)..
- Sutherland, Rebecca, David Trembath, Marie Antoinette Hodge, Veronica Rose, and Jacqueline Roberts. "Telehealth and autism:

16. Are telehealth language assessments reliable and feasible for children with autism?." International journal of language & communication disorders 54, no. 2 (2019): 281-291.
17. "Structured analysis of the retina," <http://www.ces.clemson.edu/ahoover/stare/>, accessed on May 15, 2018.
18. Gong, Chen, N. Benjamin Erichson, John P. Kelly, Laura Trutoiu, Brian T. Schowengerdt, Steven L. Brunton, and Eric J. Seibel. "RetinaMatch: Efficient Template Matching of Retina Images for Teleophthalmology." IEEE Transactions on Medical Imaging (2019).
19. J.-M. Morel and G. Yu, "Asift: A new framework for fully affine invariant image comparison," SIAM journal on imaging sciences, vol. 2, no. 2, pp. 438–469, 2009.

#### AUTHORS PROFILE



**B. Sivaranjani**, Ph.D. Scholar, Tirupur Kumaran College for Women, Tirupur(TN) and also working as a Assistant Professor, Faculty of Computer Science, Dr.N.G.P. Arts and Science college, Coimbatore(TN). She has more than 12 years of experience in teaching field. Her expertise and research interest in Pattern Recognition (Image Processing).



**Dr. C. Kalaiselvi**, Head and Professor, Dept of Computer Applications, Tirupur Kumaran College for Women, Tirupur(TN). She had qualified with SET and Ph.D. She has more than 20 years of experience in teaching and research field. Her expertise and research interest in Networking, Digital Image Processing and Data mining.